2038 *Inorg. Chem.* **2010**, *49*, 2038–2046
DOI: 10.1021/ic901250z

Inorganic Chemistry
Article

Computational Study of Methane C−H Activation by First-Row Late Transition Metal $L_nM{=}E$ (M: Fe, Co, Ni) Complexes

Aaron W. Pierpont and Thomas R. Cundari*

Department of Chemistry and Center for Advanced Scientific Computing and Modeling (CASCaM), University of North Texas, P.O. Box 305070, Denton, Texas 76203-5070

Received June 30, 2009

Methane functionalization via $L_nM{=}E$ active species (L_n = β-diketiminate, dihydrophosphinoethane; M = Fe−Ni, E = NCF_3, NCH_3, O) through a hydrogen atom abstraction (HAA)/radical rebound (RR) mechanism is calculated to be thermodynamically and kinetically feasible. The enthalpies of each reaction decrease in the order Fe > Co > Ni and with the proximity of CF_3 supporting ligand substituents ("fluorination") to the metal center. For HAA, lower abstraction enthalpies were calculated for L_n = β-diketiminate and E = NCF_3 rather than dhpe and NCH_3, respectively, whereas the opposite trend was found for RR enthalpies. The overall functionalization thermodynamics were optimal for L_n = β-diketiminate and E = NCH_3, with similar enthalpies for E = O when M = Ni. The HAA kinetics further implicate fluorinated (β-diket)Ni=O as the most promising methane functionalization complexes, with calculated activation barriers as low as 8.1 kcal mol^{-1}.

Introduction

Activation and functionalization of C−H bonds in hydrocarbons remains a vibrant field of chemical research in part because of the wealth of novel chemical transformations possible. As natural gas consists mostly of methane, selective C−H activation (or partial oxidation) could be a major route toward more valuable chemicals such as methanol. Despite the great potential for the production of functionalized organic compounds directly from hydrocarbons (as opposed to, for example, intervening reforming steps that first convert hydrocarbons into synthesis gas) on an industrial scale, the inertness of the C−H bond often necessitates that high temperatures and pressures be employed in catalysis.[1] Also, selectivity for desired partial oxidation products (such as methanol) versus more extensively oxidized products has proven difficult to achieve. This fundamental chemical drawback has thus prompted extensive research on the development of transition metal catalysts capable of selectively functionalizing the C−H bond (i.e., C−H + E → C−E−H; E = functional group) under mild conditions, even though discovery of such experimental systems that are catalytic (as opposed to stoichiometric) remains relatively rare.

One of the fruits of research on C−H bond activation has been the emergence over the last two decades of multiply bonded transition metal complexes capable of C−H activation and now encompassing examples for much of the 3d transition series. While early (typically with the metal in an oxidation state that renders a formally d^0 electronic configuration) transition metal complexes of this class are well-known, such as the Ti- and Zr-imide systems of Wolczanski, most are coordinatively unsaturated, highly reactive putative intermediates that have been characterized only in the form of dimers,[2] "solvent-trapped" complexes,[3] Lewis base and alkyne adducts,[4] and so forth. The C−H activation products, amide complexes, of these early metal imide complexes have proven to be too stable with respect to the release of functionalized products, for example, via C−N reductive elimination, to form amines. By contrast, the late transition metal congeners such as carbenes[5] and imides[5−7] of Ni and Cu are capable of activating C−H bonds *in addition* to being excellent catalysts for C−H functionalization. At the very least, these two criteria (proclivity toward both C−H bond activation and kinetically and thermodynamically accessible functionalization steps) must be met to design an energetically feasible hydrocarbon functionalization catalytic cycle.

Recent and pertinent experimental reports that satisfy the first criterion (i.e., C−H bond activation) include the nickel β-diketiminate complex $[Me_3NN]Ni{=}NAd$ (Ad = 1-adamantyl), which

*To whom correspondence should be addressed. E-mail: t@unt.edu.

(1) Labinger, J. A.; Bercaw, J. E. *Nature* **2002**, 507–514.
(2) Cummins, C. C.; Schaller, C. P.; Van Duyne, G. D.; Wolczanski, P. T.; Chan, E. A.-W.; Hoffmann, R. *J. Am. Chem. Soc.* **1991**, *113*, 2985–2994.
(3) Cummins, C. C.; Baxter, S. M.; Wolczanski, P. T. *J. Am. Chem. Soc.* **1988**, *110*, 8731–8733.
(4) Bennett, J. L.; Wolczanski, P. T. *J. Am. Chem. Soc.* **1997**, *119*, 10696–10719.
(5) Waterman, R.; Hillhouse, G. L. *J. Am. Chem. Soc.* **2003**, *125*, 13350–13351.
(6) Shay, D. T.; Yap, G. P. A.; Zakharov, L. N.; Rheingold, A. L.; Theopold, K. H. *Angew. Chem., Int. Ed.* **2005**, *44*, 1508–1510.
(7) Mindiola, D. J.; Hillhouse, G. L. *J. Am. Chem. Soc.* **2001**, *123*, 4623–4624.

 Published on Web 08/21/2009

was shown by Warren and co-workers to activate the C_{sp3}-H bond of 1,4-cyclohexadiene (CHD) to afford [Me_3NN]-Ni-NHAd.[8] Other late metal imides such as $Tp^{tBu,Me}$Co=NAd ($Tp^{tBu,Me}$ = hydrido-*tris*(3-^{t}Bu, 5-Me-pyrazolyl)borate) undergo intramolecular C−H activation.[6] A joint theoretical/experimental study has indicated that L^{Me}Fe=NAd (L^{Me} = 2,4-*bis*-(2,6-diisopropylphenylimino)pent-3-yl) exhibits both intermolecular C−H activation (the aforementioned bond of CHD), as well as room-temperature intramolecular C−H activation, both proceeding through hydrogen atom abstraction (HAA) pathways.[9] Interestingly, in the latter study, a combination of kinetics, density functional calculations, and spectroscopy implied that spin state and coordination number changes had substantial impact on C−H activating ability. This observation raises the possibility of control of the catalytic cycle for hydrocarbon functionalization through rational (but not onerous) ligand modification.

The second criterion (facile functionalization chemistry) has been achieved by the group transfer reactions of late transition metal complexes supported by chelating phosphine ligands. For example, Hillhouse et al.[5] reported the aziridination of ethylene by transfer of an NAr group from (dtbpe)Ni=NAr (dtbpe = 1,2-bis(di-*tert*-butylphosphino)-ethane; Ar = 2,6-diisopropylphenyl) to the olefin. Another recent report by the Warren and Cundari groups implicated β-diketiminate copper-nitrenes in the amination of sp^3 C−H bonds.[10] Taken together, these examples raise important questions: To what extent are late 3d block multiply bonded complexes, fully satisfying one of the above criteria, amenable to the other for C−H bonds? Additionally, what is the impact of ligand modification upon the kinetics of important activation and functionalization steps within a hydrocarbon functionalization catalytic cycle?

In this work, we seek to address these questions with a computational study of C−H activation/functionalization properties of catalysts of the form L_nM=E, where L_n is a parent β-diketiminate or dhpe (dhpe = 1,2-bis(dihydrophosphino)ethane) supporting ligand (vide infra), M is a middle to late 3d transition metal (Fe, Co, Ni), and E an activating ligand at which the initial C−H activation takes place (O, NCH_3, NCF_3). The substrate methane is chosen to rigorously test the activity of such potential catalysts, given the relatively large C−H bond dissociation enthalpy (BDE) of methane (105 kcal mol^{-1})[11] in comparison to other hydrocarbons and its importance as the main component of natural gas.

We assume a mechanism that involves hydrogen atom abstraction (HAA) (L_nM=E + CH_4 → L_nM−EH + •CH_3) followed by radical rebound (RR) (L_nM−EH + •CH_3 → $L_nM(CH_3EH)$) as the overall reaction mechanism, a choice motivated by several factors. First, our previous work on Ni complexes indicates that CHD C_{sp3}-H activation via HAA is the most favored pathway.[12] Although it is claimed in one of

Scheme 1. Idealized Catalytic Cycle for Methane Functionalization

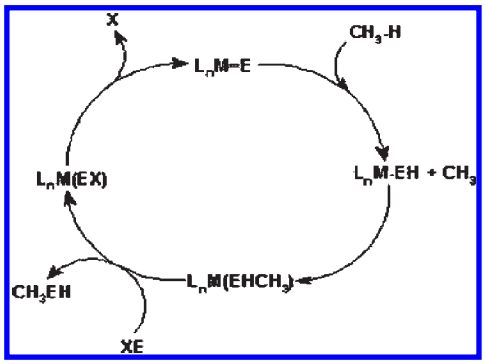

our recent computational studies of methane C−H activation with a (dhpe)Ni complex that attempts to find a HAA transition state (TS) converged to that for [1 + 2] insertion, only the reaction on the singlet potential energy surface (PES) was considered in that earlier study.[13] However, subsequent calculations at the same level of theory (B3LYP/CEP-31G(d)) confirmed that not only was the triplet PES the true ground state for C−H activation but also the triplet HAA TS was successfully located (as opposed to the singlet, which converges to the [1 + 2] insertion TS from the same initial geometry as the triplet) and the corresponding C−H activation barrier was about 8.9 kcal/mol lower than that for [1 + 2] insertion on the singlet PES. Second, the conversion of methane to methanol at both the Fe=O active site of the biologically ubiquitous Cytochrome P450 enzymes[14] as well as the Fe(μ-O)$_2$Fe intermediate of methane monooxygenase[15] are generally accepted to proceed through a HAA/RR mechanism. Third, both experimental and computational evidence implicate a HAA/RR pathway in the permanganate catalyzed oxidation of alkyl and aryl substrates to corresponding alcohols, aldehydes, and ketones.[16] Fourth, this pathway permits the dissection of the individual energy components as the M=E bond changes from formal double to formal single (HAA) and from the latter to dative (RR). Finally, in light of the coordinated $L_nM(CH_3EH)$ product, a link is forged between this mechanism and another to regenerate the L_nM=E active species and thus form a complete catalytic cycle for C−H activation (Scheme 1).

This cycle utilizes group transfer reagents of the form XE, which effectively displace the functionalized hydrocarbon ($L_nM(CH_3EH)$ + XE → $L_nM(EX)$ + CH_3EH) followed by decomposition and release of X ($L_nM(EX)$ → L_nM=E + X). Such mechanisms have been addressed computationally by Cundari et al.[12,13] and Hall and co-workers,[17] and experimentally by Ison et al.[18] Previous computational work in our group[13] along with experimental work[5,19,20] has demonstrated

(8) Kogut, E.; Wiencko, H. E.; Zhang, L.; Cordeau, D. E.; Warren, T. H. *J. Am. Chem. Soc.* **2005**, *127*, 11248–11249.
(9) Eckert, N. A.; Vaddadi, S.; Stoian, S.; Lachicotte, R. J.; Cundari, T. R.; Holland, P. L. *Angew. Chem., Int. Ed.* **2006**, *45*, 6868–6871.
(10) Badiei, Y. M.; Dinescu, A.; Dai, X.; Palomino, R. M.; Heinemann, F. W.; Cundari, T. R.; Warren, T. H. *Angew. Chem., Int. Ed.* **2008**, *47*, 9961–9964.
(11) Ruscic, B.; Litorja, M.; Asher, R. L. *J. Phys. Chem. A* **1999**, *103*, 8625–8633.
(12) Cundari, T. R.; Jimenez-Halla, J. O. C.; Morello, G. R.; Vaddadi, S. *J. Am. Chem. Soc.* **2008**, *130*, 13051–13058.
(13) Cundari, T. R.; Pierpont, A. W.; Vaddadi, S. *J. Organomet. Chem.* **2007**, *692*, 4551–4559.
(14) Meunier, B.; de Visser, S. P.; Shaik, S. *Chem. Rev.* **2004**, *104*, 3947–3980.
(15) Basch, H.; Mogi, K.; Musaev, D. G.; Morokuma, K. *J. Am. Chem. Soc.* **1999**, *121*, 7249–7256.
(16) (a) Strassner, T.; Houk, K. N. *J. Am. Chem. Soc.* **2000**, *122*, 7821–7822. (b) Lam, W. W. Y.; Yiu, S. M.; Lee, J. M. N.; Yau, S. K. Y.; Kwong, H. K.; Lau, T. C.; Liu, D.; Lin, Z. *J. Am. Chem. Soc.* **2006**, *128*, 2851–2858.
(17) Wu, H.; Hall, M. B. *J. Am. Chem. Soc.* **2008**, *130*, 16452–16453.
(18) Ison, E. A.; Cessarich, J. E.; Travia, N. E.; Fanwick, P. E.; Abu-Omar, M. M. *J. Am. Chem. Soc.* **2007**, *129*, 1167–1178.
(19) Walstrom, A. N.; Fullmer, B. C.; Fan, H.; Pink, M.; Buschhorn, D. T.; Caulton, K. G. *Inorg. Chem.* **2008**, *47*, 9002–9009.
(20) Waterman, R.; Hillhouse, G. L. *J. Am. Chem. Soc.* **2008**, *130*, 12628–12629.

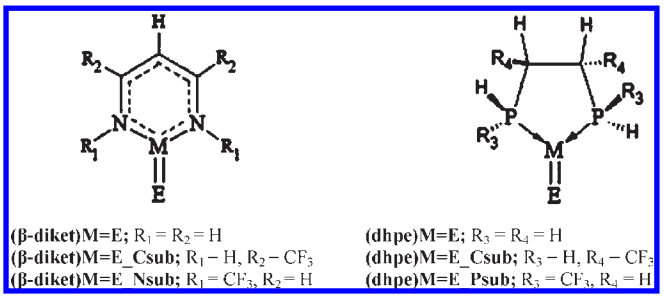

Figure 1. Supporting ligand (L_n) fluorination patterns and nomenclature.

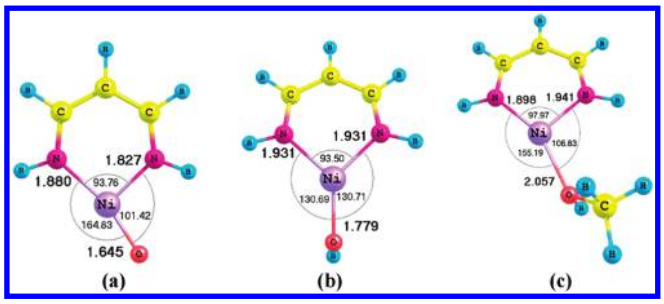

Figure 2. B3LYP/6-311+G(d) optimized geometries of (a) ^{2}(β-diket)Ni=O, (b) ^{3}(β-diket)Ni−OH, and (c) ^{2}(β-diket)Ni(CH_3OH). Ni−N and Ni−O bond lengths (**bold**) in Å and all angles in degrees.

regeneration of (dhpe)Ni=NR from (dhpe)Ni complexes via the well-known[21] imido-group transfer property of organic azides (RN_3; E = NR, X = N_2) (yielding the corresponding (dhpe)Ni=NR) to be low-barrier, thermodynamically favorable processes. Furthermore, one of the results of azide decomposition of $Cp_2Ta(Me)$-N_3Ph by Bergman et al.[22] suggests an acceleration of the decomposition rate by electron-withdrawing R groups. On the basis of these considerations, three activating ligands (E) for L_nM=E were modeled: O, NCH_3, and NCF_3.

In one of our group's more recent computational studies on the C−H activation, within the framework of the preceding mechanism, of CHD with both (dtbpe)Ni=NAr and (dfmpe)Ni=NAr (dfmpe = *bis*(di(trifluoromethyl)phosphino)ethane; Ar = 2,6-diisopropylphenyl), the thermodynamics of both HAA and RR became more feasible on replacing dtbpe with dfmpe.[12] Thus, supporting ligand (L_n) electronegativity effects on both energy components will be gauged by symmetrically substituting both the dhpe and the β-diketiminate peripheries with CF_3 groups. The substitution patterns along with their corresponding nomenclatures used herein are illustrated in Figure 1.

Computational Methods

All calculations were performed upon neutral species using the Gaussian 03 suite of programs[23] with the B3LYP hybrid density functional method.[24] Despite the previous use of the 6-31G(d) basis set for a catalytically related regeneration reaction (viz. organoazide decomposition),[13] it was deemed prudent in the present study to include diffuse functions for a more adequate description of the highly electron-withdrawing CF_3-substituted ligands. Thus, the B3LYP/6-311+G(d) level of theory was used for all calculations reported herein.

Optimized geometries and TSs were confirmed by the presence of zero and one imaginary frequencies, respectively, in the calculated energy Hessian. Thermochemistry was determined at 298.15 K and 1 atm using unscaled B3LYP/6-311+G(d) vibrational frequencies.

Results and Discussion

1. Geometries and Ground Spin States. For the (β-diket)Fe=E, (β-diket)Fe-EH, and (β-diket)Fe(CH_3EH) species, the ground spin states were quartet, quintet, and quartet, respectively. Triplet, quartet, and triplet ground states were found for the corresponding Co sequence with the exception of quintets for (β-diket)Co=NCH_3_Nsub, (β-diket)Co=O, (β-diket)Co=O_Csub, (β-diket)Co=Nsub (cf. Figure 1) and a doublet for (β-diket)Co-$NHCF_3$. The ground spin states for the Ni series were doublet, triplet, and doublet with the exception of quartet (β-diket)Ni=NCF_3_Nsub. The optimized geometry of a representative L_nM=E [^{2}(β-diket)Ni=O] species is shown in Figure 2a (cf. Figure 1 for notation), and has (like the other metal complexes discussed here) a metal coordination geometry that is trigonal planar or nearly so. The ground state multiplicities found for the (β-diket)M=E systems are consistent with those determined in a (CASPT2)/VDZP study of similar Fe^{III}(diiminato)(NPh) and Ni^{III}(diiminato)(NPh) complexes (quartet and doublet, respectively; diiminato = [$(N(Ph)CH)_2CH]^-$); although the ground state of Co^{III}(diiminato)(NPh) was calculated to be a singlet, two low-energy triplet states below 0.15 eV (3.5 kcal mol^{-1}) were predicted.[25] Representative structures of a RR product [^{3}(β-diket)Ni−OH] and a coordinated hydrocarbon product [^{2}(β-diket)-Ni(CH_3OH) are shown in Figure 2, panels b and c, respectively.

With the neutral (dhpe) supporting ligand, the optimized ground-state (dhpe)Fe=E, (dhpe)Fe-EH, and (dhpe)Fe-(CH_3EH) complexes had quintet, quartet, and triplet spin states, respectively, with the exception of the (dhpe)-Fe=NCH_3, (dhpe)Fe=NCH_3_Csub, and (dhpe)Fe=NCH_3_Psub triplets. The corresponding (dhpe)Co sequence was doublet, triplet, and doublet, with the exception of quartet oxo species (E: =O, =O_Csub, =O_Psub). Lastly, a triplet, doublet, singlet sequence was found for the respective (dhpe)Ni complexes. Representative structures of a (dhpe) catalyst [^{2}(dhpe)Co=NCH_3], RR product [^{3}(dhpe)Co-$NHCH_3$], and coordinated hydrocarbon product [^{2}(dhpe)Co($NH(CH_3)_2$)] are shown in Figures 3a−c, respectively. The optimized geometries of the remaining complexes are given in the Supporting Information.

For each of the three forms of the catalyst active species, the DFT-optimized geometry about the metal center was found to range from Y-shape to T-shape, the latter particularly manifest in Figure 2a for ^{2}(β-diket)-Ni=O and Figure 2c for ^{2}(β-diket)Ni(CH_3OH) (N−Ni−O angles ("Tee" angles) = 164.83° and 155.19°, respectively) and in Figure 3c for ^{2}(dhpe)Co($NH(CH_3)_2$) (P−Co−N angle = 151.32°). A T-shape geometry is not

(21) Cenini, S.; Gallo, E.; Caselli, A.; Ragaini, F.; Fantauzzi, S.; Piangiolino, C. *Coord. Chem. Rev.* **2006**, *250*, 1234–1253.
(22) Proulx, G.; Bergman, R. G. *Organometallics* **1996**, *15*, 684–692.
(23) Frisch, M. J.; et al.*Gaussian 03*, Revision C.02; Gaussian, Inc.: Wallingford, CT, 2004.
(24) (a) Becke, A. D. *J. Chem. Phys.* **1993**, *98*, 1372–1378. (b) Becke, A. D. *J. Chem. Phys.* **1993**, *98*, 5648–5652.
(25) Ghosh, A.; Gonzalez, E.; Tangen, E.; Roos, B. O. *J. Phys. Chem. A* **2008**, *112*, 12792–12798.

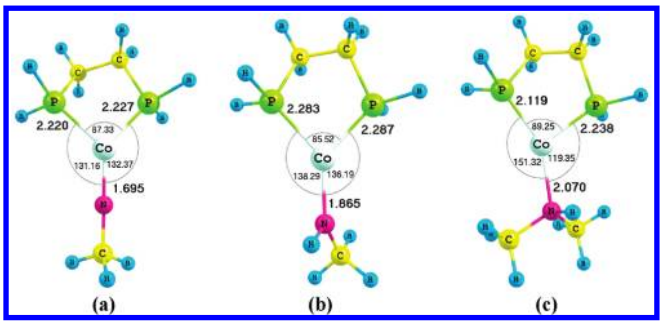

Figure 3. B3LYP/6-311+G(d) optimized geometries of (a) ^{2}(dhpe)-Co=NCH_3, (b) ^{3}(dhpe)Co-$NHCH_3$, and (c) ^{2}(dhpe)Co$(NH(CH_3)_2)$. Co−P and Co−N bond lengths (**bold**) in Å and all angles in degrees.

unprecedented for three-coordinate complexes of the late 3d metals, pertinent examples of which include L^{Me}Ni=NAd (Ad = 1-adamantyl; L^{Me} = methyl analogue of L^{tBu} (vide supra)) and [Me_2NN]Ni(2,4-lutidine) X-ray crystal structures ([Me_2NN] = 2,4-*bis*(2,6-dimethylphenylimido)pentane).[8] Furthermore, in a recent computational-experimental study, a T-shape was found for the X-ray crystal geometry of the Ni(I) complex L^{Me}Ni(CO), which was attributed to electronic structure effects.[26]

Nevertheless, several complexes were found in which the ground state geometry differs markedly from that of a low-lying excited state. For instance, the optimized geometry of the ground state triplet of (β-diket)Co=NCF_3 shows a Y-shape whereas that of the quintet, with an energy gap of only 1.0 kcal mol^{-1}, has a T-shape ("Tee" angle = 149.82°). The ground state geometries in these cases should thus be considered tentative until higher levels of theory (and more sterically demanding model ligands) are used to determine the true nature of the ground state for more experimentally apropos complexes.

Aside from Y- and T-shape structures, the three (dhpe)Ni=O catalysts (E = O, O_Csub, O_Nsub; cf. Figure 1) converged to rather unusual stationary points. Geometry optimization starting from a Y-shaped [(dhpe)-Ni=O] guess yielded the corresponding (dhpeO)Ni species, where the supporting ligand is a phosphine/phosphine oxide (dhpeO = $PH_2CH_2CH_2PH_2$(=O)), with the P=O bond coordinated to Ni in an η^2-PO fashion (Figure 4), in agreement with previous optimizations at a lower level of theory (B3LYP/CEP-31G(d)).[27] Interestingly, Pd(II) was shown by Grushin[28] to catalyze formation of the related monoxide dppeO (dppeO = $PPh_2CH_2CH_2PPh_2$(=O)) from dppe under alkaline conditions. Although these serendipitous computational predictions of coordinated dhpeO ligands undoubtedly have important implications for such transformations given the number of metal-oxo complexes capable of converting phosphines to phosphine oxides[29] (we are currently carrying out calculations for related *bis*-phosphine monoxide Ni complexes), the three (dhpeO)Ni systems will not be given further consideration here.

2. Thermodynamics. 2.1. Effect of Metal. The reaction enthalpies for the overall reaction (L_nM=E + CH_4 → L_nM(CH_3EH); L_n = substituted/unsubstituted β-diketiminate or dhpe; M = Fe, Co, Ni; E = NCH_3, NCF_3, O) are presented in Table 1. For each activating/supporting ligand (E/L_n) combination, the reaction enthalpies are calculated to decrease in the order Fe > Co > Ni, with the most favorable enthalpies for Ni catalyst models. Despite the exothermicity of most of the reactions, a few of those featuring Fe and Co (highlighted in **bold** in Table 1) are endothermic. Furthermore, for certain ligand combinations, the spread of the energies for different metals is larger than 30 kcal mol^{-1}. In particular, the reaction enthalpies for (β-diket)M=O where M is Fe, Co, or Ni are calculated to be 13.9, −1.6, and −22.0 kcal mol^{-1}, respectively, thus spanning ~36 kcal mol^{-1} as one progresses from left to right in the 3d series from Fe to Co to Ni. Three other catalytic systems for which the calculated metal "spreads" are > 30 kcal mol^{-1} are (β-diket)M=NCF_3, (β-diket)M=O_Csub, and (β-diket)M=O_Nsub (30.0, 34.8, and 35.3 kcal mol^{-1}, respectively). The calculations thus highlight and to some extent quantify the substantial impact that the metal plays in determining the thermodynamics of E group transfer.

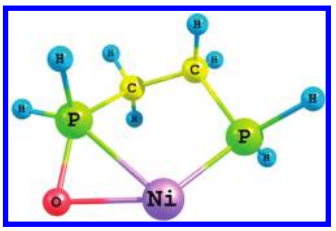

Figure 4. B3LYP/6-311+G(d) optimized geometry of (dhpeO)Ni.

Table 1. Overall Reaction Enthalpies (kcal mol^{-1}) for (L_nM=E + CH_4 → L_nM(CH_3EH))[a]

	β-diketiminate			dhpe		
E	Fe	Co	Ni	Fe	Co	Ni
NCH_3	**0.8**	−15.0	−21.6	**0.4**	−5.2	−22.7
NCH_3_Csub	−10.1	−21.6	−31.0	−5.3	−9.8	−27.3
NCH_3_(Nsub/Psub)	−18.2	−29.7	−40.7	−9.3	−12.1	−29.5
NCF_3	**8.7**	−9.3	−21.3	**15.5**	**7.2**	−11.5
NCF_3_Csub	−4.4	−18.4	−30.3	**5.3**	**1.0**	−18.4
NCF_3_(Nsub/Psub)	−14.6	−27.5	−43.6	**2.6**	−3.2	−22.1
O	**13.9**	−1.6	−22.0	**21.1**	**7.3**	*b*
O_Csub	**3.5**	−10.3	−31.3	**11.7**	−0.2	*b*
O_(Nsub/Psub)	−4.1	−20.5	−39.4	**8.3**	−3.5	*b*

[a] Endothermic reactions are highlighted in **bold**. [b] (dhpe)Ni=O and related complexes are unstable; the stationary points consist of the 'O' activating ligand bound to a dhpe 'P' atom and hence the thermodynamics from an oxo starting material could not be determined.

In light of the foregoing observations, we decided to further probe the energetics of the overall methane functionalization reaction by dissecting it into two components: hydrogen atom abstraction (HAA: L_nM=E + CH_4 → L_nM−EH + •CH_3) followed by RR (RR: L_nM−EH + •CH_3 → L_nM(CH_3EH)). The reaction enthalpies for HAA are given in Table 2, and it is seen that for all metal/ligand combinations, they are endothermic with ΔH_{HAA} indicating less endothermic abstractions from Fe to Ni, the sole exception being those for ^{3}(β-diket)Co=NCF_3 and ^{2}(β-diket)Ni=NCF_3 (7.4 and 7.9 kcal mol^{-1}, respectively). Despite our recent findings of exothermic HAA reactions

(26) Eckert, N. A.; Dinescu, A.; Cundari, T. R.; Holland, P. L. *Inorg. Chem.* **2005**, *44*, 7702–7704.
(27) Cundari, T. R.; Vaddadi, S. *J. Mol. Struct. THEOCHEM* **2006**, *801*, 47–53.
(28) (a) Grushin, V. V. *Organometallics* **2001**, *20*, 3950–3961. (b) Grushin, V. V. *J. Am. Chem. Soc.* **1999**, *121*, 5831–5832.
(29) Holm, R. H. *Chem. Rev.* **1987**, *87*, 1401–1449.

Table 2. HAA Enthalpies (kcal mol^{-1}) for $L_nM{=}E + CH_4 \rightarrow L_nM{-}EH + {\bullet}CH_3$

	β-diketiminate			dhpe		
E	Fe	Co	Ni	Fe	Co	Ni
NCH_3	19.8	19.0	18.6	24.2	20.9	16.6
NCH_3_Csub	19.3	18.3	18.0	24.8	19.8	16.3
NCH_3_(Nsub/Psub)	17.1	15.6	13.4	23.7	21.7	16.2
NCF_3	9.2	7.4	7.9	17.1	8.9	6.9
NCF_3_Csub	7.3	5.8	5.7	13.8	7.6	6.2
NCF_3_(Nsub/Psub)	6.0	3.8	0.3	14.0	7.5	5.0
O	12.6	10.2	3.6	21.5	9.8	*a*
O_Csub	9.7	8.6	1.0	18.6	7.0	*a*
O_Nsub	7.3	7.0	0.1	18.6	7.2	*a*

[a] Note that (dhpe)Ni=O and related complexes are unstable at the B3LYP/6-311+G(d) level of theory. See footnote b in Table 1 and attendant text.

Table 3. E—H BDEs ($L_nM{-}EH \rightarrow L_nM{=}E + {\bullet}H$; kcal/mol)

	β-diketiminate			dhpe		
E	Fe	Co	Ni	Fe	Co	Ni
NCH_3	82.9	83.7	84.0	78.5	81.8	86.1
NCH_3_Csub	83.4	84.4	84.7	77.9	82.9	86.4
NCH_3_(Nsub/Psub)	85.6	87.1	89.3	78.9	81.0	86.5
NCF_3	93.5	95.2	94.8	85.6	93.8	95.8
NCF_3_Csub	95.4	96.9	96.9	88.9	95.0	96.5
NCF_3_(Nsub/Psub)	96.7	98.9	102.3	88.7	95.2	97.7
O	90.1	92.5	99.1	81.2	92.9	*a*
O_Csub	93.0	94.1	101.7	84.1	95.7	*a*
O_(Nsub/Psub)	95.4	95.6	102.6	84.0	95.5	*a*

[a] Note that (dhpe)Ni=O and related complexes are unstable at the B3LYP/6-311+G(d) level of theory. See footnote b in Table 1 and attendant text.

for 1,4-cyclohexadiene (CHD),[12] the opposite finding in this study can be explained by further decomposing the HAA reaction into a homolytic C−H bond dissociation reaction ($CH_4 \rightarrow H{\bullet} + {\bullet}CH_3$) followed by E−H bond formation ($L_nM{=}E + {\bullet}H \rightarrow L_nM{-}EH$), the energetics of the latter concomitantly yielding E−H bond dissociation energies. The B3LYP/6-311+G(d) calculated methane C−H BDE is 102.7 kcal mol^{-1}, which compares favorably with the experimental value of 105 kcal/mol.[11] The calculated E−H BDEs (from the enthalpy of $L_nM{-}EH \rightarrow L_nM{=}E + {\bullet}H$) are presented in Table 3. Comparing the energetics of both reactions, it is clear that for each abstraction reaction the strength of the E−H bond formed is not sufficient to offset that of the methane C−H bond, one of the strongest bonds of any hydrocarbon. By contrast, the calculated C_{sp3}-H BDE of CHD at this level of theory is only 70.4 kcal mol^{-1}, compared with the recent value of 76.9 ± 0.7 kcal mol^{-1} reported by DeYonker et al.[29] from a combination of experiments and high-level, ab initio calculations. Not only do these observations explain the endothermicity of the HAA reactions with methane, but also the exothermicities of similar reactions with CHD as substrate.[12]

Among all E/L_n combinations, the E−H bond strength increases monotonically from Fe to Ni (E−H BDE: Ni > Co > Fe; Table 3). Additionally, the choice of E = NCF_3 for Fe and Co gives the strongest E−H bond (E−H BDE (M = Fe, Co): NCF_3 > O > NCH_3) whereas O−H bonds were strongest for Ni (E−H BDE (M = Ni): O > NCF_3 > NCH_3). Just as fluorinated activating ligands enhance the E−H BDE, so too does supporting ligand fluorination and proximity of such fluorination to the metal center *for β-diketiminate species* (E−H BDE: $L_nM{=}E$_Nsub > $L_nM{=}E$_Csub > $L_nM{=}E$); dhpe complexes are less sensitive to fluorination, which does not alter their E−H BDEs in a systematic fashion (Table 3).

Table 4. RR Enthalpies (kcal mol^{-1}) for $L_nM{-}EH + {\bullet}CH_3 \rightarrow L_nM(CH_3EH)$

	β-diketiminate			dhpe		
E	Fe	Co	Ni	Fe	Co	Ni
NCH_3	−19.0	−34.0	−44.2	−23.8	−26.1	−39.2
NCH_3_Csub	−29.4	−39.9	−49.0	−30.1	−29.6	−43.6
NCH_3_(Nsub/Psub)	−35.3	−45.4	−54.1	−33.0	−33.8	−45.7
NCF_3	−0.5	−16.7	−29.2	−1.6	−1.7	−18.4
NCF_3_Csub	−11.7	−24.2	−36.1	8.5	−6.7	−24.5
NCF_3_(Nsub/Psub)	−20.6	−31.3	−44.0	−11.4	−10.7	−27.1
O	1.3	−11.8	−25.6	−0.3	−2.4	*a*
O_Csub	−6.2	−18.9	−32.2	−6.8	−7.2	*a*
O_(Nsub/Psub)	−11.4	−27.6	−39.4	−10.4	−10.7	*a*

[a] Note that (dhpe)Ni=O and related complexes are unstable at the B3LYP/6-311+G(d) level of theory. See footnote to Table 1 and attendant text.

Although exothermic CHD abstractions are predicted for all of the active species in Table 3 utilizing either our calculated CHD BDE (70.4 kcal mol^{-1}) or that of DeYonker et al.[30] (76.9 ± 0.7 kcal mol^{-1}), with the weakest E−H bond calculated for ^{4}(dhpe)Fe=$NHCH_3$_Csub (E−H BDE = 77.9 kcal mol^{-1}), this is not the case for the stronger C−H bond of methane. Only three of the catalytic systems were found to have E−H BDEs > 100 kcal mol^{-1} and thus strong enough to permit a thermodynamically viable CH_4 HAA reaction with $L_nM{=}E$ active species: ^{3}(β-diket)-Ni=$NHCF_3$_Nsub, ^{3}(β-diket)Ni=OH_Csub, and ^{3}(β-diket)Ni=OH_Nsub (E−H BDE: 102.3, 101.7, and 102.6 kcal mol^{-1}, respectively; cf. 102.7 kcal mol^{-1} methane C−H BDE).

The thermodynamics of the second component reaction, RR, are listed in Table 4. As with the overall reaction, along with the HAA component, the RR enthalpies decrease in the order Fe > Co > Ni. Thus, the most thermodynamically favorable processes for methane C−H activation with the $L_nM{=}E$ active species considered are those incorporating Ni.

To explore the thermodynamic trend for RR in more detail, it is instructive to focus on the change in formal electron configurations. For the Ni(II) amides [(β-diket)Ni-EH] and Ni(I) amides [(dhpe)Ni-EH], the formal transition metal electron configurations change from $3d^8$ to $3d^9$ and $3d^9$ to $3d^{10}$, respectively, upon RR to form the corresponding amines. It would intuitively seem as though the RR thermodynamic trend is caused by the extent to which the $n = 3$ shell is completely filled. Hence, analogous calculations were performed for (β-diket)Cu-EH and (dhpe)Cu-EH (E = NCH_3, NCF_3). The RR reactions of the latter species (nominally $3d^{10}$ to $3d^{10}4s^1$; $\Delta_{RR}(NCH_3) = -19.1$ kcal mol^{-1}; $\Delta_{RR}(NCF_3) = 5.4$ kcal mol^{-1}) were the least thermodynamically favorable with respect to their earlier 3d transition metal counterparts (cf. Table 4) whereas the opposite was found for the (β-diket)Cu species ($3d^9$ to $3d^{10}$; $\Delta_{RR}(NCH_3) = -51.4$ kcal mol^{-1}; $\Delta_{RR}(NCF_3) = -39.8$ kcal mol^{-1}). This observation is in agreement with the

(30) Gao, Y.; DeYonker, N. J.; Garrett, E. C., III; Wilson, A. K.; Cundari, T. R.; Marshall, P. *J. Phys. Chem. A* **2009**, *113*, 6955–6963.

hypothesis that the thermodynamic favorability of RR correlates with the filling of the 3d manifold.

2.2. Effect of Activating Group (E). Of all the catalysts considered, those incorporating the oxo ligands ($L_nM{=}O$) displayed the least favorable thermodynamics in terms of the overall HAA/RR reaction (ΔH_{tot}: O > NCF_3 > NCH_3) with the exception of the ^{2}(β-diket)-Ni=O and ^{4}(dhpe)Co=O series (all three L_n substitution patterns) both of which entail a change in formal electron configuration of $3d^7$ to $3d^9$ over the course of the reaction and display strikingly similar thermodynamics to their ^{2}(β-diket)Ni=NCF_3 and ^{2}(dhpe)Co=NCF_3 counterparts, respectively (Table 1). For the HAA component, the thermodynamic preference is intermediate that of the two imido activating ligands (ΔH_{HAA}: NCH_3 > O > NCF_3) whereas the RR to $L_nM(OHCH_3)$ is the least favored (ΔH_{RR}: OH > $NHCF_3$ > $NHCH_3$). Once again, the (β-diket)Ni=O and (dhpe)Co=O series evade these trends by displaying similar thermodynamics to their NCF_3 counterparts (cf. Tables 2 and 4).

For the methyl-imido active species ($L_nM{=}NCH_3$), the effect of replacement of the activating group with its fluorinated counterpart ($L_nM{=}NCF_3$) is to make the overall HAA/RR reaction less favorable by no more than 7.9 kcal mol^{-1} and 15.2 kcal mol^{-1} for L_n = β-diketiminate and dhpe, respectively (Table 1), the lone exception being ^{2}(β-diket)Ni=NCH_3_Nsub (ΔH_{tot}: ^{2}(β-diket)Ni=NCH_3_Nsub > ^{4}(β-diket)Ni=NCF_3_Nsub by 2.9 kcal mol^{-1}). However, analysis of the enthalpies of each component reaction reveals the opposite trend for HAA: the abstractions for $L_nM{=}NCF_3$ are 11.3 ± 1.6 kcal mol^{-1} less endothermic, and thus more favorable, on average than for $L_nM{=}NCH_3$ (Table 2).

To probe the source of the increase in HAA potency upon fluorination, test calculations were performed for the simple abstraction reactions $^3NCH_3 + CH_4 \rightarrow {}^2NHCH_3 + {\bullet}CH_3$ and $^3NCF_3 + CH_4 \rightarrow {}^2NHCF_3 + {\bullet}CH_3$. The former, non-fluorinated abstraction reaction was calculated to be 10.3 kcal mol^{-1} more endothermic than the latter, thus mirroring the thermodynamic preference for fluorinated amine activating ligands in their L_nM bound counterparts. In light of the relatively small effect of changing the metal and supporting ligand (Section 2.3) of the imido catalysts (Table 1), the HAA enthalpies of $L_nM{=}NCH_3$ are thus deemed to be most sensitive to fluorination of the activating ligand.

The enthalpic trend for imido catalysts in the overall reaction (ΔH_{tot}: NCF_3 > NCH_3) is mirrored by the RR reactions, with the rebounds for fluorinated catalysts 18.4 ± 4.0 kcal mol^{-1} more endothermic than those of the non-fluorinated catalysts (Table 4). Thus, while fluorination of the imido activating ligand may be thermodynamically favorable for HAA (by 11.3 ± 1.6 kcal mol^{-1}), it is more than offset by the preference for non-fluorination during RR, yielding an overall thermodynamic predilection for non-fluorinated imido catalysts. Proceeding in an analogous fashion with the simple HAA reactions, two simple rebound reactions were considered: $^2NHCH_3 + {\bullet}CH_3 \rightarrow NH(CH_3)_2$ and $^2NHCF_3 + {\bullet}CH_3 \rightarrow NH(CH_3)(CF_3)$. However, not only is the fluorinated rebound 9.5 kcal mol^{-1} more *exothermic* than the former ($NHCH_3$ > $NHCF_3$), in direct contrast to their L_nM bound counterparts, but unlike HAA, both the metal and supporting ligand (vide infra) have a pronounced effect on the RR thermodynamics (Table 4).

2.3. Effect of Supporting Ligand (L_n) Substitution. The formal oxidation state of the metal imposed by either the neutral dhpe or the monoanionic β-diketiminate supporting ligand has a significant effect on the reaction energetics. The overall reactions for the higher oxidation states of β-diketiminate ((β-diket)M^{III}(E) as opposed to (dhpe)M^{II}E) are less endothermic than their lower oxidation state dhpe counterparts by 2.9−21.5 kcal mol^{-1} depending on M and E (Table 1). Despite the lone exception of $L_nFe{=}NCH_3$ (ΔH_{tot}: ^{4}(β-diket)Fe=NCH_3 > ^{3}(dhpe)Fe=NCH_3), the difference in reaction enthalpy is only 0.4 kcal mol^{-1} for this system.

Although the same thermodynamic trend is followed for the HAA component (ΔH_{HAA}: (β-diket) < (dhpe) by 0.2−11.3 kcal mol^{-1}), there are more exceptions of this nature. The ^{2}(β-diket)Ni=NCF_3, ^{2}(β-diket)Ni=NCH_3, ^{2}(β-diket)Ni=NCH_3_Csub, ^{5}(β-diket)Co=O, and ^{5}(β-diket)Co=O_Csub active species display abstractions more endothermic than their dhpe counterparts by 0.4−1.7 kcal mol^{-1} (Table 2). These in turn are compensated by more exothermic (by 5.0−11.7 kcal mol^{-1}) RR reactions, thus yielding an overall thermodynamic preference for the (β-diket) catalysts in these cases. Interestingly, the same trend *and* exceptions (in terms of activating ligands) found for HAA are calculated for RR, with (ΔH_{RR}: (β-diket) < (dhpe)) by 1.0−20.6 kcal mol^{-1}, a range similar to that of the overall reaction, and (ΔH_{RR}: (β-diket) > (dhpe)) by 0.6−4.8 kcal mol^{-1} for $L_nFe{=}NCF_3$, $L_nFe{=}NCH_3$, $L_nFe{=}NCH_3$_Csub, $L_nFe{=}O$, and $L_nFe{=}O$_Csub.

In a parallel fashion with the aforementioned HAA trend exceptions, those for the rebound reactions are compensated by 5.5−8.9 kcal mol^{-1} for the corresponding abstractions. However, even though the rebound with ^{5}(β-diket)Fe=$NHCH_3$ is disfavored by 4.8 kcal mol^{-1} over that for ^{4}(dhpe)Fe=$NHCH_3$, the 4.4 kcal mol^{-1} preference for abstraction with ^{4}(β-diket)Fe=NCH_3 over ^{3}(dhpe)Fe=NCH_3 is not sufficient to overcome the poorer thermodynamics of the rebound, yielding an overall reaction that is 0.4 kcal mol^{-1} more endothermic for ^{4}(β-diket)Fe=NCH_3 than ^{3}(dhpe)Fe=NCH_3. This is the source of the lone exception (ΔH_{tot}: (β-diket) > (dhpe); cf. Table 1) in the thermodynamics of the overall reaction. Thus, in general, $L_nM{=}E$ active species with higher metal oxidation states (L_n = β-diket) give more favorable methane functionalization thermodynamics than those with lower oxidation states (dhpe).

Just as it is possible to alter the energetics of the activation and rebound reactions by a suitable change in supporting ligand (and possibly metal formal oxidation state), the effect of "tuning" a given supporting ligand by adding functional groups ($-CF_3$ in the present case) may also be calculated. The choice of $-CF_3$ groups is particularly attractive as they have been shown to fortify supporting ligands against oxidation.[31,32] The range in reaction enthalpies for each three-member set of ligand

(31) Laitar, D. S.; Mathison, C. J. N.; Davis, W. M.; Sadighi, J. P. *Inorg. Chem.* **2003**, *42*, 7354–7356.
(32) Hamilton, C. W.; Laitar, D. S.; Sadighi, J. P. *Chem. Commun.* **2004**, 1628–1629.

Table 5. Reaction Enthalpy Ranges (kcal mol^{-1}) for $-CF_3$ Substitution Patterns of the β-Diketiminate (dhpe) Supporting Ligand

	NCH_3	NCF_3	O
		Overall	
Fe	19.0 (9.6)	23.3 (12.9)	18.0 (12.8)
Co	14.7 (6.9)	18.2 (10.4)	18.9 (10.8)
Ni	15.1 (6.8)	22.3 (10.6)	17.4[a]
		HAA	
Fe	2.7 (1.1)	3.2 (3.1)	5.3 (2.9)
Co	3.4 (1.9)	3.6 (1.4)	3.2 (2.8)
Ni	5.2 (0.4)	7.6 (1.9)	3.5[a]
		RR	
Fe	16.3 (9.2)	20.1 (9.8)	18.0 (12.8)
Co	11.4 (7.7)	14.6 (9.0)	18.9 (10.8)
Ni	9.9 (6.5)	14.8 (8.7)	13.8[a]

[a] Note that (dhpe)Ni=O and related complexes are unstable at the B3LYP/6-311+G(d) level of theory. See footnote b in Table 1 and attendant text.

substitution patterns (Figure 1) is given in Table 5 and is equivalent to the difference of highest and lowest magnitude reaction enthalpy of each triumvirate. For instance, of the [^{4}(β-diket)Fe=NCH_3, ^{4}(β-diket)Fe=NCH_3_Csub, ^{4}(β-diket)Fe=NCH_3_Nsub] group, the HAA enthalpies are 19.8, 19.3, and 17.1 kcal mol^{-1}, respectively (Table 2), yielding a 2.7 kcal mol^{-1} range for this set. Without exception, the (β-diket) complexes are more thermodynamically sensitive to CF_3 substitution ("fluorination" in this work) than those of dhpe, as indicated by the relatively larger enthalpy ranges of the former (Table 5) by an average of 8.6, 2.3, and 6.2 kcal mol^{-1} for the overall reaction, HAA, and RR, respectively While the HAA reaction for catalysts of both supporting ligands exhibits little sensitivity to fluorination ((β-diket): 2.7−7.6 kcal mol^{-1}; (dhpe): 0.4−3.1 kcal mol^{-1}), the effect is more pronounced with RR ((β-diket): 9.9−20.1 kcal mol^{-1}; (dhpe): 6.5−12.8 kcal mol^{-1}), the latter reaction thus being the dominant contributor to the CF_3 sensitivity of the overall reaction ((β-diket): 14.7−23.3 kcal mol^{-1}; (dhpe): 6.8−12.9 kcal mol^{-1}).

In general, the HAA/RR and overall reactions become more exothermic with the proximity of the CF_3 groups to the metal center (ΔH: L_nM=E > L_nM=E_Csub > L_nM=E_(Nsub/Psub); Tables 1, 2, and 4) with the exception of the HAA reaction for the four triumvirates of ^{3}(dhpe)Fe=NCH_3, ^{2}(dhpe)Co=NCH_3, ^{5}(dhpe)Fe=O, and ^{4}(dhpe)Co=O (Table 2) with respect to HAA. Nevertheless, these exceptions may be trivial as the HAA enthalpy ranges for these sets are 1.1, 1.9, 2.9, and 2.8 kcal mol^{-1}, respectively, reflecting the relative insensitivity of the HAA reaction in conjunction with the dhpe supporting ligand to fluorination. The robustness imparted by supporting ligand fluorination is also supported experimentally, where for instance C−H activation of alkyl and aryl substrates was enhanced with increasing fluorination of the porphyrin ring of metalloporphyrin oxygenation catalysts.[33,34] Additionally, these observations are reflected in our previous study of CHD functionalization. Upon replacing the P-bound ^{t}Bu groups of (dtbpe)Ni=NAr with CF_3 to give (dfmpe)-Ni=NAr, both the calculated CHD HAA and the RR enthalpies decreased by 4.4 and 32.9 kcal mol^{-1}, respectively.[12] For the analogous (dhpe)Ni=NCH_3 and (dhpe)Ni=NCF_3 complexes of the present study, fluorination (CF_3) at the P-atoms (yielding (dhpe)Ni=NCH_3_Psub and (dhpe)Ni=NCF_3_Psub) results in a slightly more favorable methane HAA enthalpy by 0.4 and 1.9 kcal mol^{-1}, respectively, with a greater enhancement by 6.5 (E = NCH_3) and 8.7 (E = NCF_3) kcal mol^{-1} for $\cdot CH_3$ RR. The most probable explanation for the apparently higher sensitivity of CHD functionalization thermodynamics to (dtbpe)Ni=NAr fluorination is the greater extent of fluorination (substitution with four CF_3 groups) with respect to the methane functionalization systems (two CF_3 groups).

3. Kinetics. Given the relatively favorable thermodynamics afforded by L_nNi=E complexes, the scope of the kinetic analysis will be limited to Ni systems. The HAA activation enthalpies are given in Table 6. For the E = NCH_3 complexes (NCH_3, NCH_3_Csub, NCH_3_(Nsub/Psub)), it is seen that the calculated kinetics ($\Delta H^{\ddagger}_{act}$) show little sensitivity to fluorination of the supporting ligand, with the exception of fluorination at the N atoms for ^{2}(β-diket)Ni=NCH_3_Nsub (smaller barrier by ~3 kcal mol^{-1}). Comparing the two supporting ligands with E = NCH_3, a slight kinetic preference is found for the lower oxidation state (dhpe) species (~25 kcal mol^{-1} vs ~23 kcal mol^{-1} for β-diketiminate and dhpe, respectively). The optimized geometry of a representative TS ([^{2}(β-diket)Ni−N(CH_3)···H···CH_3]‡) is shown in Figure 5a.

Switching to the E = NCF_3 complexes (NCF_3, NCF_3_Csub, NCF_3_(Nsub/Psub)) from the NCH_3 complexes lowers the calculated C−H activation barriers by 8.3−7.2 kcal mol^{-1} and 6.0−2.6 kcal mol^{-1} for L_n = β-diketiminate and dhpe, respectively. Unlike the NCH_3 ligands, there is no clear kinetic preference between low (dhpe) and high (β-diketiminate) oxidation states for the NCF_3 ligands, the average barrier being ~18 kcal mol^{-1} in both cases. Furthermore, fluorination of the supporting ligands does not change the kinetics in a systematic fashion. Figure 5b shows the optimized geometry of a representative transition structure ([^{2}(β-diket)Ni−N(CF_3)···H···CH_3]‡).

The E = O complexes (O, O_Csub, O_(Nsub/Psub)) have barriers 2.1−8.0 kcal mol^{-1} below those of the β-diketiminate NCF_3 catalysts. Among the three activating ligands employed, the choice of E = O in conjunction with a β-diketiminate supporting ligand (corresponding dhpe complexes not considered; see Section 1) yields the best kinetics for methane C−H activation, with the optimized geometry of a representative TS ([^{2}(β-diket)-Ni−O−H−CH_3]‡) given in Figure 5c. Fluorination of the supporting ligand in such complexes lowers the kinetic barrier to HAA by up to 7.5 kcal mol^{-1}, with the kinetics improving with the proximity of CF_3 groups to Ni.

Also included in Table 6 for each reaction is the calculated percentage M=E elongation, defined as the ratio of the difference in M=E bond length in the L_nM=E

(33) Lyons, J. E.; Ellis, P. E., Jr; Myers, H. K., Jr. *J. Catal.* **1995**, *155*, 59–73.
(34) Porheil, E.; Bondon, A.; Leroy, J. *Tetrahedron Lett.* **1998**, *39*, 4829–4830.

Table 6. HAA Activation Barriers (kcal mol^{-1}) for (L_nNi=E + CH_4 → [L_nNi—E···H···CH_3]‡)

	β-diketiminate		dhpe	
E	$\Delta H^{\ddagger}_{act}$	% M=E elongation	$\Delta H^{\ddagger}_{act}$	% M=E elongation
NCH_3	26.5	60	22.6	76
NCH_3_Csub	26.1	61	22.6	77
NCH_3_(Nsub/Psub)	23.3	78	22.4	77
NCF_3	17.7	77	17.3	68
NCF_3_Csub	18.8	68	16.6	67
NCF_3_(Nsub/Psub)	16.1	64	19.8	74
O	15.6	81	*a*	*a*
O_Csub	13.6	83	*a*	*a*
O_(Nsub/Psub)	8.1	77	*a*	*a*

[a] Note that (dhpe)Ni=O and related complexes are unstable at the B3LYP/6-311+G(d) level of theory. See footnote b in Table 1 and attendant text.

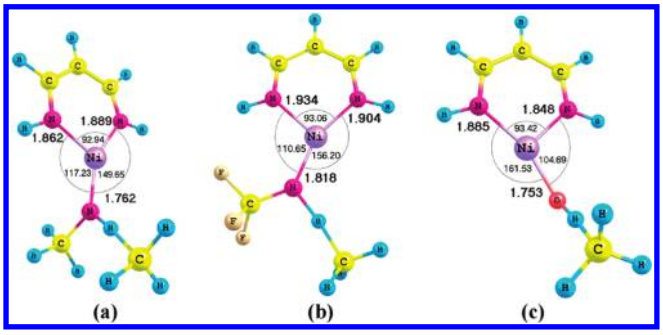

Figure 5. B3LYP/6-311+G(d) optimized HAA TS structures for reaction of methane with (a) ^{2}(β-diket)Ni=NCH_3, (b) ^{2}(β-diket)Ni=NCF_3, and (c) ^{2}(β-diket)Ni=O. Ni−N and Ni−O bond lengths (**bold**) in Å and all angles in degrees.

catalyst and TS to the difference in M=E bond length in L_nM=E and L_nM−EH, which gives an indication of the "lateness" of each TS:

$$\%\text{M=E elongation} = \{([\text{M—E}]_{TS} - [\text{M—E}]_{react}) / ([\text{M—E}]_{prod} - [\text{M—E}]_{react})\} \times (100)$$

According to the % M=E elongation ("elongation") values in Table 6, all of the transition structures may be classified as late, that is, the calculated M=E bond length in the TS is closer to the L_nM−EH intermediate than that of the L_nM=E reactant. For L_n = β-diketiminate, the increase in M=E elongation in the order NCH_3 < NCF_3 < O (with the exception of the N substituted supporting ligands) correlates with the decrease in $\Delta H^{\ddagger}_{act}$ along the same ligand series ($\Delta H^{\ddagger}_{act}$: NCH_3 > NCF_3 > O). However, the opposite elongation trend is seen for L_n = dhpe with smaller elongations found for smaller barriers. Thus, these observations suggest that in the high oxidation state (i.e., L_n = β-diketiminate) L_nM=E catalysts, lower methane C−H activation barriers correspond to later TSs for hydrogen atom abstraction whereas for the lower oxidation state catalysts (dhpe), later TSs correlate with larger HAA barriers.

Summary and Conclusions

In conclusion, methane activation via L_nM=E is both thermodynamically and kinetically feasible given an appropriate choice of transition metal, supporting ligand, and activating ligand. Hydrogen atom abstraction (HAA) (L_nM=E + CH_4 → L_nM−EH + •CH_3) was found to be most thermodynamically feasible for the latest of the 3d transition metals studied here (ΔH_{HAA}: M = Fe > Co > Ni; Table 2). Fluorination of imido activating ligands (ΔH_{HAA}: E = NCH_3 > O > NCF_3) resulted in less endothermic abstractions by 11.3 ± 1.6 kcal mol^{-1} than for their non-fluorinated L_nM=NCH_3 counterparts (Table 2) with additional thermodynamic preferences for higher oxidation states (ΔH_{HAA}: L_n = dhpe > β-diket) and proximity of supporting ligand fluorination to the metal center (ΔH_{HAA}: unsub > C_sub > (N/P)_sub; Figure 1).

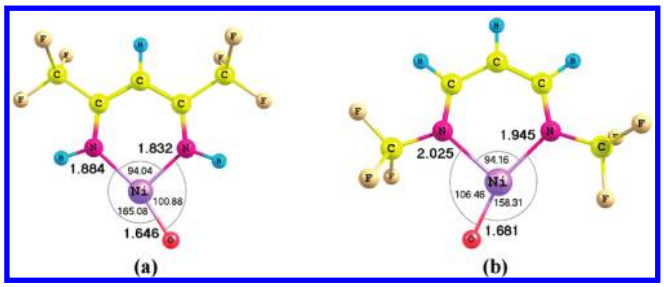

Figure 6. B3LYP/6-311+G(d) optimized geometries of most promising methane HAA/RR active species (a) ^{2}(β-diket)Ni=O_Csub and (b) ^{4}(β-diket)Ni=O_Nsub. Ni−N and Ni−O bond lengths (**bold**) in Å and all angles in degrees.

Although the same trends hold for RR (L_nM−EH + •CH_3 → L_nM(CH_3EH)), fluorination of the imido activating ligand resulted in a *less* exothermic RR (ΔH_{RR}: E = O > NCF_3 > NCH_3; Table 4). In fact, the RR thermodynamic preference for E = NCH_3 is sufficient to offset the HAA preference for E = NCF_3, giving an overall preference for the former activating ligand in the joint HAA/RR reaction.

Altogether, the joint HAA/RR reaction (L_nM=E + CH_4 → L_nM(CH_3EH)) becomes less endothermic with both the "lateness" of the transition metal (ΔH_{tot}: M = Fe > Co > Ni; Table 1) and higher oxidation states (ΔH_{tot}: L_n = dhpe > β-diket) of the active species. Additionally, lower overall reaction enthalpies were found with the proximity of supporting ligand fluorination to the metal center, with the β-diketiminate ligands exhibiting the greatest sensitivity in this regard (Table 5). Even though the thermodynamics were most favorable for the NCH_3 activating ligand (ΔH_{tot}: E = O > NCF_3 > NCH_3), the most exothermic functionalizations predicted in this work, for fluorinated (β-diket)Ni=NCH_3 species (−31.0 and −40.7 kcal mol^{-1} for the Csub and Nsub isomers, respectively; Table 1), are similar in magnitude to those of the corresponding oxo species (−31.3 and −39.4 kcal mol^{-1} for (β-diket)Ni=O_Csub and (β-diket)-Ni=O_Nsub, respectively).

In terms of HAA kinetics for the Ni complexes, each abstraction TS may be classified as "late" (Table 6) and the barriers decrease along the activating ligand series ($\Delta H^{\ddagger}_{act}$: E = NCH_3 > NCF_3 > O). Fluorination of the β-diketiminate supporting ligand in (β-diket)Ni=O further lowers the barrier by up to 7.5 kcal mol^{-1} for (β-diket)Ni=O_Nsub, for which the calculated methane C−H activation barrier (8.1 kcal mol^{-1}) was the lowest of all active species considered.

Thus, among the systems investigated here, the most promising C−H activation catalysts for a HAA/RR mechanism have active species of the form ^{2}(β-diket)Ni=O_Csub

and ^{4}(β-diket)Ni=O_Nsub, the optimized structures of which are given in Figure 6. We are currently performing computational work on the group transfer reactions ($L_nM(CH_3EH) + XE \rightarrow L_nM{=}E + CH_3EH + X$; cf. Scheme 1) for a suitable choice of group transfer reagent (XE) using Ni(III) and Ni-oxo catalysts, homogeneous and heterogeneous, which will complete the desired catalytic cycle for the transformation $CH_4 + XE \rightarrow CH_3EH + X$.

Acknowledgment. The authors acknowledge the continued financial support from the National Science Foundation of the computational facilities at UNT (CRIF, CHE-0741936). This research is supported by a DOE grant to T.R.C. (DEFG02-03ER15387). A.W.P. acknowledges the UNT Tolouse Graduate School for a College of Arts and Sciences Graduate Research Fellowship.

Supporting Information Available: Cartesian coordinates of all species used to obtain thermodynamic and kinetic data along with their spin multiplicities and full citation for ref 23. This material is available free of charge via the Internet at http://pubs.acs.org.